Association of quantifiable prostate MRI parameters with any and large cribriform pattern in prostate cancer patients undergoing radical prostatectomy

Neslisah Seyrek [a,b,*], Eva Hollemans [a], Ivo G. Schoots [b,1], Geert J.L.H. van Leenders [a,1]

[a] Department of Pathology, Erasmus MC Cancer Institute, University Medical Centre, Rotterdam, The Netherlands
[b] Department of Radiology and Nuclear Medicine, Erasmus MC Cancer Institute, University Medical Centre, Rotterdam, The Netherlands

ABSTRACT

Purpose: Cribriform pattern has recently been recognized as an important independent risk factor for prostate cancer (PCa) outcome. This study aimed to identify the association of quantifiable prostate magnetic resonance imaging (MRI) parameters with any and large cribriform pattern at radical prostatectomy (RP) specimens.
Methods: Preoperative prostate MRI's from 188 men undergoing RP between 2010 and 2018 were retrospectively acquired. RP specimens of the patients were revised for Gleason score (GS), and presence of any and large cribriform pattern. MRI parameters such as MRI visibility, PI-RADS score, lowest apparent diffusion coefficient (ADC) value, lesion size, and radiologic extra-prostatic extension (EPE) were reviewed. The association of prostate MRI parameters for presence of any and large cribriform pattern at RP was analysed using logistic regression.
Results: 116/188 (61.7%) PCa patients had any cribriform and 36/188 (19.1%) large cribriform pattern at RP. 171/188 (91.0%) men had MRI-visible lesions; 111/116 (95.7%) tumours with any and 36/36 (100%) with large cribriform pattern were visible at MRI. PCa with any and large cribriform pattern both had lower ADC values than those without (p < 0.001). In adjusted analysis, lowest ADC value was as an independent predictor for any cribriform (Odds Ratio (OR) 0.2, 95% Confidence Interval (CI) 0.1–0.8; p = 0.01) and large cribriform pattern (OR 0.2, 95% CI 0.1–0.7; p = 0.01), while other parameters were not.
Conclusions: The majority of PCa with cribriform pattern at RP were visible at MRI, and lowest ADC value was an independent predictor for both any and large cribriform pattern.

1. Introduction

Prostate cancer (PCa) is amongst the most common cancers worldwide impacting on healthcare and quality of life. Risk stratification is critical in PCa management, as not all men with PCa need treatment. The biopsy-derived Gleason score (GS)/ Grade group (GG) is the most important parameter for PCa risk stratification. Men with GG1 (GS 3 + 3) tumours are mostly eligible for surveillance, while patients with GG3-

5 cancer generally undergo active treatment [1–3]. Despite being considered as intermediate risk, men with GG2 (GS 3 + 4) cancer have variable outcome. Active treatment is offered to most of these patients, while an increasing number of GG2 men is now also considered to be candidate for surveillance [4].

Invasive cribriform and intraductal carcinoma (CR/IDC) have been recognized as independent pathological factors for shorter biochemical recurrence-, metastasis- and disease specific-free survival [5–8].

Furthermore, in RP specimens large expansile cribriform pattern is associated with more frequent extra-prostatic extension, positive lymph nodes and biochemical recurrence than small cribriform pattern [9]. Therefore presence of cribriform architecture in biopsy GG2 men is nowadays an important exclusion criterion for active surveillance [4].

Multiparametric magnetic resonance imaging (mpMRI) has rapidly been adopted in PCa diagnosis because of its high sensitivity for clinically significant PCa. Apart from providing lesion-based assessment via the Prostate Imaging-Reporting and Data Systems (PI-RADS) score, it also supports pre-operative decision-making in PCa patients [10,11]. The accuracy of PCa detection significantly increases with mpMRI-directed targeted biopsy and upgrading of biopsy specimens is less likely with this approach [12–14]. Recent publications showed that cribriform architecture occurs more frequently in men with PI-RADS score 5 lesions [15,16]. Furthermore, mpMRI Apparent Diffusion Coefficient (ADC) values have been inversely correlated with tumour aggressiveness [17].

PCa is a heterogeneous and multifocal disease, which often leads to biopsy sampling errors and underestimation of true tumour aggressiveness. This is not only reflected in Gleason grading discordances, but also in the detection of cribriform pattern which is missed in about half of cases [18,19]. Since GG2 men without cribriform pattern (favourable intermediate risk) are considered eligible for active surveillance, false cribriform-negative biopsies could result in undertreatment of the PCa patients. Therefore, identification of cribriform pattern is important for accurate individual risk stratification and treatment.

Up to now, few studies have focused on identifying mpMRI parameters for overall cribriform pattern, without discriminating large and small cribriform size. The aim of this study is to identify independent pre-operative mpMRI parameters associated with any and large cribriform pattern in PCa patients who underwent RP for their disease.

2. Materials and methods

2.1. Patient selection

This study included 188 consecutive patients who had undergone mpMRI and RP for prostate adenocarcinoma without prior therapy in our institute between 2010 and 2018. The study was approved by the institutional Medical Research Ethics Committee (MEC-2020-0998).

2.2. Pathological evaluation

RP specimens were fixed in neutral-buffered formalin, after which they were sectioned transversely and entirely embedded for diagnostic purposes. All RP specimens were reviewed in joint sessions by two investigators (EH, GvL), blinded to clinical outcome. For each specimen, the following features were recorded: GS and GG according to the 2014 ISUP/ 2016 WHO recommendations, pT-stage according to the American Joint Committee on Cancer (AJCC) TNM 8th edition, surgical margin status and presence of cribriform architecture. Cribriform architecture encompassed both invasive cribriform and intraductal carcinoma (IDC) lesions. Large cribriform pattern was defined as having a diameter of at least twice the size of adjacent pre-existent normal glands, and could either represent one large well defined cribriform field or a confluent cribriform area. In case of multifocality, we only monitored the characteristics of the index tumour defined as the tumour with the highest grade, stage, or volume. Tertiary patterns occupying < 5% of the tumour volume and IDC were not included in the GG.

2.3. MRI protocol

3.0 Tesla mpMRI (Discovery MR750, General Electrics, WI, USA) was used in 169 (89.9%) men prior to RP, and 1.5 Tesla (Discovery MR450, General Electrics, WI, USA) in 19 (10.1%) patients. 3.0 Tesla and 1.5 Tesla mpMRI's were both included in order to increase the sample size.

Each patient received protocolized intramuscular 20 mg Buscopan (Boehringer, Ingelheim, Germany) administration before imaging. Acquired mpMRI images were taken compliant to PI-RADS 2019 guidelines with T2 weighted (T2W), diffusion weighted (DWI), and dynamic contrast-enhanced (DCE) sequences (Supplementary Table 1).

2.4. Radiological evaluation

Pre-operative mpMRI's were reviewed in joint sessions by NS (researcher, 2 years of experience) and IS (radiologist, 13 years of experience), both blinded to clinical and pathological outcome, according to PI-RADS v2.1 (2019) guidelines [20]. In case of multifocality, only the index lesion with highest PI-RADS score was taken into account. In case of multiple lesions with similar PI-RADS scores, the lesion with the highest diameter was registered. Quantifiable lesion parameters such a) longest diameter of the lesion, b) capsular contact length, c) radiological stage, and d) minimum ADC values were assessed for the index tumour with a unit of measurement of $10^{-6}mm^2/s$. Lowest ADC values were assessed manually by the regional measurement tools of VuePACS server (Carestream/Philips, Best, The Netherlands), at the region of interest, where index tumour location overlapped on axial T2W, DWI and ADC images. Then, the measurements were validated by computerized calculation. ADC images of 34 patients (18.1%) could not be retrieved due to low imaging quality of DWI sequences and these patients were excluded from analysis of ADC values. In addition to PI-RADS score, the following quantifiable extra-prostatic extension (EPE) parameters acknowledged by the American College of Radiology (ACR) were assessed in axial T2W images: a) capsular abutment, b) capsular bulging, c) capsular irregularity, d) capsular breakthrough, e) radius of invasion, f) neurovascular bundle asymmetry, g) seminal vesicle invasion, and h) bladder neck invasion. Information collected from quantifiable EPE parameters were gathered in a 4-tier EPE Likert scale of 1) not likely EPE, 2) equivocal (EPE < 1 mm), 3) EPE likely (between 1 and 3 mm), and 4) highly likely (EPE > 3 mm)[20].

2.5. Statistical analysis

Continuous variables with normal distribution were analysed using the Student's *t*-test and continuous variables without normal distribution using Mann-Whitney or Kruskal-Wallis test. Pearson's chi square (χ^2) or Fisher's exact test was used to compare categorical parameters. The predictive value of pre-operative mpMRI parameters for both any and large cribriform pattern at RP was estimated by uni- and multi-variable logistic regression analysis. Results were considered significant when the two-sided p-value was < 0.05. Statistics were performed with IBM SPSS Statistics 25 (IBM, Chicago, IL, USA) and R version 4.1.1 (R, Vienna, Austria).

3. Results

3.1. Clinicopathological characteristics

The median age at time of RP was 65.7 years (Interquartile Range (IQR) 60.9–70.4) and the median prostate specific antigen (PSA) level was 8.7 ng/mL (IQR 6.4–14.8). Out of 188 RP specimens, cribriform architecture was observed in 116 (61.7%) men, of whom 36/116 (19.1%) had large cribriform pattern (Table 1). Cribriform architecture was observed in 16.0% GG1, 57.1% GG2, 100% GG3, 80.0% GG4, and 78.9% GG5 tumours. Large cribriform pattern was observed in 0% GG1, 7.6% GG2, 51.7% GG3, 40.0% GG4, and 47.4% GG5 tumours. Pathological tumour stage was 46.8% pT2, 39.9% pT3a, and 13.3% pT3b. Positive surgical margins (PSM) and metastatic disease at pelvic lymph node dissection (PLND) were observed in 37.7% and 9.6%, respectively. GG was associated with age, cribriform architecture, pT-stage and lymph node metastasis.

Table 1
Clinicopathologic characteristics of the radical prostatectomy (RP) patients stratified by Grade Group (GG).

	Total n = 188	GG1 n = 25	GG2 n = 105	GG3 n = 29	GG4 n = 10	GG5 n = 19	p-value
Age (IQR)	65.7 (60.9–70.4)	61.7(57.3–66.9)	65.9 (61.2–69.4)	65.6 (59.7–70.0)	68.9 (65.3–72.4)	70.5 (64.7–74.1)	0.003[a]
PSA (IQR)	8.7 (6.4–14.8)	7.8(5.6–10.2)	8.9 (6.5–14.0)	11.6 (6.8–19.0)	11.2 (5.0–17.0)	8.40 (5.4–17.6)	0.20[a]
Any CR	116 (61.7%)	4 (16.0%)	60 (57.1%)	29 (100%)	8 (80.0%)	15 (78.9%)	<0.001[b]
Large CR	36 (19.1%)	0 (0%)	8 (7.6%)	15 (51.7%)	4 (40.0%)	9 (47.4%)	<0.001[b]
pTNM							<0.001[b]
T2	88 (46.8%)	18 (72.0%)	55 (52.4%)	6 (20.7%)	5 (50.0%)	4 (21.1%)	
T3a	75 (39.9%)	7 (28.0%)	41 (39.0%)	14 (48.3%)	4 (40.0%)	9 (47.4%)	
T3b	25 (13.3%)	0 (0%)	9 (8.6%)	9 (31.0%)	1 (10.0%)	6 (31.6%)	
PSM	71 (37.7%)	8 (32.0%)	34 (32.4%)	15 (51.7%)	4 (40.0%)	10 (52.6%)	0.46[b]
LN meta	18 (9.6%)	0 (0%)	5(4.8%)	8 (27.6%)	1 (10.0%)	4 (21.1%)	0.001[b]

[a] Kruskal-Wallis test, [b]Chi-square test, IQR: Interquartile Range, PSA: Prostate specific antigen, CR: Cribriform, PSM: Positive surgical margin, LN meta: lymph node metastasis.

3.2. Quantifiable mpMR imaging characteristics

Prostate mpMRI identified 171/188 PCa's with a sensitivity of 90.9% (95% Confidence Interval (CI) 86.7–94.5). PI-RADS assessment showed 9.0% score 2, 5.9% score 3, 28.2% score 4, and 56.9% score 5. Higher PI-RADS scores were significantly associated with increasing GG (p = 0.04) and pT-stage (p < 0.001). 19.1% men had EPE Likert scale 1, 38.8% had scale 2, 24.5% scale 3, and 8.5% scale 4, respectively. Radiological tumour stage was rT2 in 65.4% and rT3 in 23.9% men, while no tumour was visible (rT1) in 10.6% men. Neither Likert scale nor radiological staging were significantly associated with GG, while tumour visibility (p = 0.001), increasing PI-RADS score (p < 0.001) and lowest ADC values (p = 0.04) all were (Supplementary Table 2).

3.3. MpMRI features of tumours with cribriform architecture

Table 2 summarizes the comparative mpMRI features of any and large cribriform lesions to the ones without these patterns. High PSAD was significantly associated with any cribriform growth (p = 0.02), while it did not reach conventional levels of significance for large cribriform pattern (p = 0.07). MpMRI identified 111 out of 116 index tumours with cribriform architecture, resulting in a detection rate of 95.7% (95% CI 89.7–98.4), and it's presence was significantly associated with mpMRI visibility (p = 0.004). Out of 116 patients with any cribriform pattern, 5 (4.3%), 6 (5.2%), 29 (25.0%), 76 (65.5%) had PI-RADS scores 2, 3, 4 and 5 (p = 0.005), respectively. As for the 36

patients with large cribriform pattern, 9 (25.0%) and 27 (75.0%) had PI-RADS score 4 and 5 (p = 0.025), respectively. Maximum diameter of the index lesion was significantly associated with large cribriform pattern (19.5 mm, IQR 14.3–25.8 versus 16.0 mm, IQR 12.2–21.2p = 0.02), but did not reach significance (p = 0.09) for presence of any cribriform pattern. EPE Likert scale was significantly associated with both any cribriform (p = 0.003) and large cribriform pattern (p = 0.005). Tumours with any and large cribriform pattern both had higher radiological T-stage (p < 0.001). Any and large cribriform positive cancers had lower (p < 0.001) ADC values on MRI than tumours without cribriform pattern. In particular, GG2patients with any (p < 0.001) and large cribriform (p = 0.04) pattern had significantly lower ADC values (Fig. 1). Among the individual quantifiable radiologic EPE parameters, capsular abutment (p = 0.02), capsular breakthrough (p = 0.002) and neurovascular bundle asymmetry (p = 0.01) were significantly associated with any cribriform pattern. Capsular abutment (p = 0.01), tumour bulging (p < 0.001), capsular line irregularity (p = 0.047), capsular contact length (p = 0.002), capsular breakthrough (p = 0.01), neurovascular bundle asymmetry (p = 0.02) and seminal vesicle invasion were all significantly associated with large cribriform pattern. The association of individual quantifiable radiologic EPE parameters with any and large cribriform are shown in Supplementary Tables 3 and 4, respectively.

Table 2
Prostate magnetic resonance imaging (MRI) parameters stratified by any cribriform and large cribriform pattern at radical prostatectomy (RP) specimen.

	No CRn = 72 (38.3%)	Any CR+n = 116 (61.7%)	p-value	Large CR-n = 152 (80.9%)	Large CR+n = 36 (19.1%)	p-value
PSAD (IQR)	0.21 (0.14–0.30)	0.26 (0.17–0.41)	0.02[a]	0.24 (0.15–0.37)	0.32 (0.20–0.39)	0.07[a]
PI-RADS			0.005[b]			0.025[b]
2	12 (16.7%)	5 (4.3%)		17 (11.2%)	0 (0.0%)	
3	5 (6.9%)	6 (5.2%)		11 (7.2%)	0 (0.0%)	
4	24 (33.3%)	29 (25.0%)		44 (28.9%)	9 (25.0%)	
5	31 (43.1%)	76 (65.5%)		80 (52.6%)	27 (75.0%)	
MRI visible	60 (83.3%)	111(95.7%)	0.004[b]	135 (88.8%)	36 (100.0%)	0.03[b]
TZ index lesion	13 (18.1%)	18 (15.5%)	0.69[c]	27 (17.8%)	4 (11.1%)	0.46[c]
Index lesion longest diameter (IQR, mm)	14.8 (11.5–20.8)	17.20 (13.1–22.1)	0.09[a]	16.0 (12.2–21.2)	19.5 (14.3–25.8)	0.02[a]
EPE Likert scale			0.003[b]			0.005[b]
no EPE	16 (22.2%)	20 (17.2%)		17 (11.2%)	0 (0.0%)	
EPE < 1 mm	31 (43.1%)	42 (36.2%)		32 (21.1%)	4 (11.1%)	
EPE 1 mm-3 mm	11 (15.3%)	35 (30.2%)		35 (23.0%)	11 (30.6%)	
EPE > 3 mm	2 (2.8%)	14 (12.0%)		8(5.2%)	8 (22.2%)	
Radiologic TNM			<0.001[b]			0.001[b]
rT1	14 (19.4%)	6 (5.2%)		20 (13.2%)	0 (0.0%)	
rT2a/b/c	49 (68.1%)	74 (63.8%)		103 (67.8%)	20 (55.6%)	
rT3a/b	9 (12.5%)	36 (31.0%)		29 (19.1%)	16 (44.4%)	
Lowest ADC (IQR, 10⁻⁶mm²/s)	691.0 (566.0–851.0)	567.0 (474.0–673.5)	<0.001[a]	631.0 (536.0–763.0)	504.0 (426.0–588.0)	<0.001[a]

[a] Kruskal-Wallis test, [b]Chi-square test, [c]Fisher's exact test, IQR: Interquartile Range, CR: Cribriform, PSAD: Prostate specific antigen density, PI-RADS: Prostate Imaging Reporting and Data System, TZ: Transitional zone, EPE: Extra-prostatic extension, ADC: Apparent iffusion coefficient.
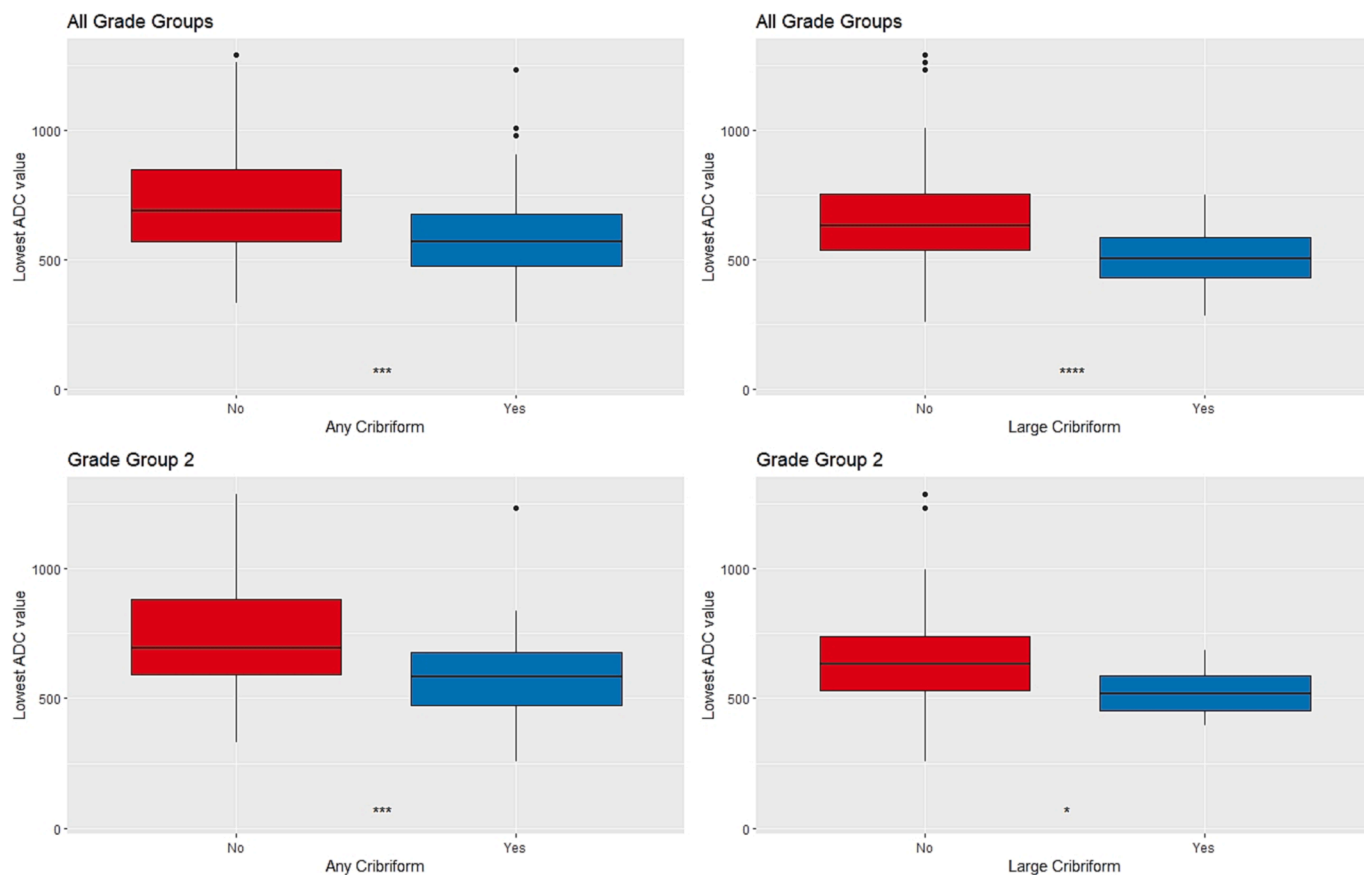
Fig. 1. Median lowest ADC values comparisons of the whole cohort (n = 188) and Grade Group 2 patients (n = 105) with any and large cribriform pattern in radical prostatectomy specimens.

3.4. Associated MRI features with cribriform architecture

In univariate logistic regression analysis prostate specific antigen density (PSAD), RP GG > 2, PI-RADS score 5, EPE > 1 mm, and lowest ADC value were all significantly associated with presence of any cribriform architecture at RP specimens (Table 3). In adjusted analysis PSAD, GG > 2 and lowest ADC value (Odds Ratio (OR) 0.2, 95% CI 0.1–0.8; p = 0.01) were all independent factors for presence of cribriform architecture while the other radiological variables were not. Similarly, PI-RADS score 5, RP GG > 2, EPE > 1 mm and lowest ADC value were all related to the presence of large cribriform pattern in univariate logistic regression analysis, while PSAD was not. In analysis adjusted for GG and radiological parameters, lowest ADC value (OR 0.2, 95% CI 0.1–0.7; p = 0.01) and GG > 2 were independent predictive factors for large cribriform pattern, while PI-RADS score 5 and EPE > 1 mm were not.

4. Discussion

In the current study, we explored the diagnostic value of mpMRI in identifying high risk PCa with any and more aggressive large cribriform pattern. According to our results, 95.7% of cribriform lesions and all large cribriform structures had PI-RADS score ≥ 3, and lowest ADC value was an independent predictive parameter for both. These findings indicate that PI-RADS score and lowest ADC values should be considered in decision-making in biopsy cribriform-negative PCa patients.

In our study, 66% of any and 75% of large cribriform tumours had PI-RADS score 5 index lesions, with the remaining 25% of large structures having PI-RADS score 4, which is comparable with other studies [21–23]. Gao et al. found PI-RADS score 5 to be an independent predictive parameter for cribriform pattern in GG2 and GG3 patients [16].

Van der Slot et al. found that PI-RADS score 5 was an independent predictive factor for upgrading biopsy GG2 men without cribriform pattern in a cohort of 283 patients [24]. In the current study, PI-RADS score 5 was predictive for any and large cribriform pattern in univariate but not in adjusted analysis. Some other groups similarly did not find a statistically significant relation between PI-RADS score 5 and cribriform architecture at RP in multivariable regression models [18,25]. The fact that PI-RADS score lost its independent predictive value in multivariable analysis could be due to our relatively small sample size. On the other hand, PI-RADS score might be related to tumour grade in general, but less to cribriform pattern in particular.

We found that ADC values in any and large cribriform PCa were significantly lower than in tumours without these patterns (Fig. 1). Lower ADC values observed in cribriform pattern may be influenced by the extent of tissue cellularity and the arrangement of malignant epithelial cells within cribriform structures, which decreases intervening stroma and vessels, and is even more aberrant within large cribriform pattern. Earlier studies demonstrate that higher ADC values were associated with less aggressive tumours [17,26]. Prendeville et al. observed significantly lower ADC values in tumours with cribriform architecture in a prospective biopsy cohort of 154 patients [15]. Arslan et al. also found that lesions with cribriform architecture had significantly lower ADC values in a RP cohort [22]. In a case-control study comparing RP GG2 patients with and without IDC, Currin et al. revealed that tumours with IDC had lower mean ADC values [27]. On the other hand, Truong et al. and Tonttila et al. concluded that there was no significant difference in ADC values of cribriform positive and negative tumours [21,23]. Since ADC maps are derived from DWI sequences, quantitative ADC values are substantially dependent on variations in b-values, utility of scanners and post-processing algorithms. Consequently, comparison of these individual studies is difficult. The

Table 3
Univariable and multivariable logistic regression analysis of predicting (a) any cribriform and (b) large cribriform pattern in radical prostatectomy (RP) patients.

a)	Univariable OR	Multivariable 95% CI	p-value	OR	95% CI	p-value
PSAD*	1.5	1.1 – 2.0	0.01	1.8	1.1 – 2.9	0.01
GG1 & GG2	Ref	Ref		Ref	Ref	
GG3 & GG4 & GG5	8.9	3.6 – 22.2	<0.001	6.0	1.9 – 17.6	0.001
PI-RADS scores 2 & 3 & 4	ref	ref		Ref	Ref	
PI-RADS score 5	2.5	1.4 – 4.6	0.002	1.0	0.4 – 2.7	0.9
EPE Likert Scale Likert Scale 1&2 (EPE < 1 mm)	Ref	Ref		Ref	Ref	
Likert Scale 3&4 (EPE > 1 mm)	2.8	1.4 – 5.9	0.004	2.6	0.9 – 7.7	0.07
Lowest ADC*	0.2	0.1 – 0.5	<0.001	0.2	0.1 – 0.8	0.01

b)	Univariable OR	Multivariable 95% CI	p-value	OR	95% CI	p-value
PSAD*	1.2	0.9 – 1.7	0.2	–	–	–
GG1 & GG2	Ref	Ref		Ref	Ref	
GG3 & GG4 & GG5	14.2	5.9 – 34.4	<0.001	9.0	3.3 – 24.8	<0.001
PI-RADS scores 2 & 3 & 4	Ref	Ref		Ref	Ref	
PI-RADS score 5	2.7	1.1 – 6.1	0.02	1.1	0.3 – 3.7	0.8
EPE Likert Scale Likert Scale 1&2 (EPE < 1 mm)	Ref	Ref		Ref	Ref	
Likert Scale 3&4 (EPE > 1 mm)	2.4	1.1 – 5.0	0.02	2.6	0.8 – 8.0	0.1
Lowest ADC*	0.2	0.1 – 0.5	<0.001	0.2	0.1 – 0.7	0.01

OR: Odds ratio, CI: Confidence interval, PSAD: Prostate specific antigen density, GG: Grade group, PI-RADS: Prostate Imaging Reporting and Data System, EPE: Extra-prostatic extension, ADC: Apparent diffusion coefficient.
*Denotes log2 conversion.

significance of these radiological variables should be investigated in larger cohorts with multivendor mpMRI scanners and protocols, and their effects should be studied in risk-stratification models.

Cribriform architecture has been recognized as an important pathological parameter for PCa outcome[28]. Specifically in biopsy GG2 patients, absence or presence of cribriform pattern is used nowadays for clinical decision-making on active treatment or surveillance [4]. Pathological detection of cribriform pattern, however, is affected by a high rate of false-negative biopsies due to sampling error [18,19,25,29]. For instance, in a study among GG2 biopsy patients, Hollemans et al. found that 40% were false-negative for any cribriform pattern and 27% for large cribriform pattern [9]. Identification of those false cribriform-negative biopsies is of clinical importance especially for biopsy GG2 men, preventing them from undertreatment. Apart from the clinical significance of PI-RADS score 5 lesions, high ADC values might point at the presence of favourable intermediate risk GG2 PCa (Fig. 2). Standardization of reporting lowest ADC value in radiological assessments will facilitate determination of optimal cut-off values for aggressive PCa, although variability in scanner devices and post-processing software might limit definition of globally applicable recommendations. Also, biopsy GG1 and GG2 men with adverse radiological parameters such as radiological EPE, low ADC values and PI-RADS score 5 may benefit from second radiological reading and confirmatory targeted and/or systematic biopsies.

The strong points of this study are the detailed review of RP specimens and mpMRI images according to contemporary guidelines. This study also has several limitations. The number of patients is limited and derived from one single centre retrospectively, limiting the power of the statistical analysis. Inclusion of index lesions only may lead to disregarding the information of additional lesions, particularly of the rare cases with lower PI-RADS scores with cribriform pattern. The use of both 3 T and 1.5 T imaging modalities, along with variations in b-values due to yearly imaging protocol updates, may have introduced some heterogeneity. Tumour locations and characteristics in the RP specimens were not spatially mapped to mpMRI images. Additionally, as a consequence of including pre-operative mpMRI's, the study cohort consisted predominantly of mpMRI visible PCa, which might have led to enrichment of cribriform lesions and over-estimation of results. Finally, since diagnostic biopsies were not available for pathological review, other potentially important pathology factors and biopsy GG could not be taken into account.

MpMRI is able to identify the vast majority of PCa with any and large cribriform pattern. Quantitative ADC value is an independent radiological parameter for both any and large cribriform architecture. These findings might support clinical decision-making in GG2 PCa patients with false cribriform-negative biopsy outcome, and decrease the risk for undertreatment of potentially aggressive disease.

Informed consent

Written informed consent was not required for this study because it concerns medical scientific research and participants are subjected to procedures or are required to follow rules of behavior.

Ethical approval

Institutional Review Board approval was obtained for this research.

CRediT authorship contribution statement

Neslisah Seyrek: Writing – original draft, Visualization, Investigation, Formal analysis. **Eva Hollemans:** Formal analysis. **Ivo G. Schoots:** Conceptualization, Methodology, Supervision. **G.J.L.H. van Leenders:** Conceptualization, Methodology, Supervision.
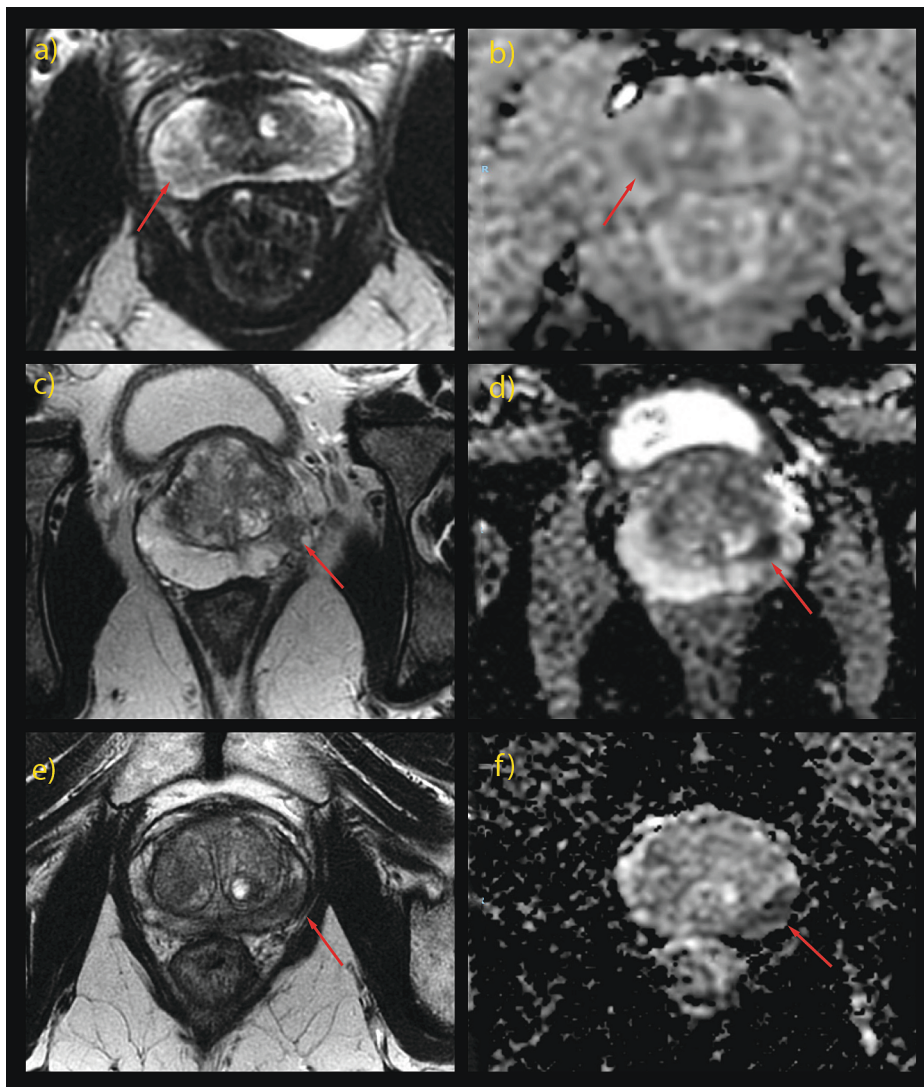
Fig. 2. Representations of prostate cancer index lesions on pre-operative MRI scans of pathological Grade Group 2 patients at radical prostatectomy specimen. PI-RADS score 3 index lesion on T2w (a) and ADC (b) images with a lowest ADC value of 940.0 10^{-6}mm^2/s without any cribriform architecture on RP. PI-RADS score 4 index lesion on T2w (c) and ADC (d) images with a lowest ADC value of 621.0 10^{-6}mm^2/s with any cribriform architecture at radical prostatectomy. PI-RADS score 5 index lesion on T2w(e) and ADC (f) images with lowest ADC value of 455.0 10^{-6}mm^2/s with large cribriform architecture at radical prostatectomy.

Declaration of Competing Interest

The authors declare that they have no known competing financial interests or personal relationships that could have appeared to influence the work reported in this paper.

Appendix A. Supplementary data

Supplementary data to this article can be found online at https://doi.org/10.1016/j.ejrad.2023.110966.

References

[1] N. Mottet, R.C.N. van den Bergh, E. Briers, T. Van den Broeck, M.G. Cumberbatch, M. De Santis, S. Fanti, N. Fossati, G. Gandaglia, S. Gillessen, N. Grivas, J. Grummet, A.M. Henry, T.H. van der Kwast, T.B. Lam, M. Lardas, M. Liew, M.D. Mason, L. Moris, D.E. Oprea-Lager, H.G. van der Poel, O. Rouvière, I.G. Schoots, D. Tilki, T. Wiegel, P.M. Willemse, P. Cornford, EAU-EANM-ESTRO-ESUR-SIOG Guidelines on Prostate Cancer-2020 Update. Part 1: Screening, Diagnosis, and Local Treatment with Curative Intent, Eur Urol 79 (2) (2021) 243–262.

[2] E. Schaeffer, S. Srinivas, E.S. Antonarakis, A.J. Armstrong, J.E. Bekelman, H. Cheng, A.V. D'Amico, B.J. Davis, N. Desai, T. Dorff, J.A. Eastham, T. A. Farrington, X. Gao, E.M. Horwitz, J.E. Ippolito, M.R. Kuettel, J.M. Lang, R. McKay, J. McKenney, G. Netto, D.F. Penson, J.M. Pow-Sang, R. Reiter, S. Richey, M. Roach Iii, S. Rosenfeld, A. Shabsigh, D.E. Spratt, B.A. Teply, J. Tward, D. A. Shead, D.A. Freedman-Cass, NCCN Guidelines Insights: Prostate Cancer, Version 1.2021, J Natl Compr Canc Netw 19 (2) (2021) 134–143.

[3] M.G. Sanda, J.A. Cadeddu, E. Kirkby, R.C. Chen, T. Crispino, J. Fontanarosa, S. J. Freedland, K. Greene, L.H. Klotz, D.V. Makarov, J.B. Nelson, G. Rodrigues, H. M. Sandler, M.E. Taplin, J.R. Treadwell, Clinically Localized Prostate Cancer: AUA/ASTRO/SUO Guideline. Part I: Risk Stratification, Shared Decision Making, and Care Options, J Urol 199 (3) (2018) 683–690.

[4] T.B.L. Lam, S. MacLennan, P.M. Willemse, M.D. Mason, K. Plass, R. Shepherd, R. Baanders, C.H. Bangma, A. Bjartell, A. Bossi, E. Briers, A. Briganti, K. T. Buddingh, J.W.F. Catto, M. Colecchia, B.W. Cox, M.G. Cumberbatch, J. Davies, N.F. Davis, M. De Santis, P. Dell'Oglio, A. Deschamps, J.F. Donaldson, S. Egawa, C. D. Fankhauser, S. Fanti, N. Fossati, G. Gandaglia, S. Gillessen, N. Grivas, T. Gross, J. P. Grummet, A.M. Henry, A. Ingels, J. Irani, M. Lardas, M. Liew, D.W. Lin, L. Moris, M.I. Omar, K.H. Pang, C.C. Paterson, R. Renard-Penna, M.J. Ribal, M.J. Roobol, M. Rouprêt, O. Rouvière, G. Sancho Pardo, J. Richenberg, I.G. Schoots, J.P. M. Sedelaar, P. Stricker, D. Tilki, S. Vahr Lauridsen, R.C.N. van den Bergh, T. Van den Broeck, T.H. van der Kwast, H.G. van der Poel, G. van Leenders, M. Varma, P. D. Violette, C.J.D. Wallis, T. Wiegel, K. Wilkinson, F. Zattoni, J.M.O. N'Dow, H. Van Poppel, P. Cornford, N. Mottet, EAU-EANM-ESTRO-ESUR-SIOG Prostate Cancer Guideline Panel Consensus Statements for Deferred Treatment with Curative Intent for Localised Prostate Cancer from an International Collaborative Study (DETECTIVE Study), Eur Urol 76 (6) (2019) 790–813.

[5] C.F. Kweldam, M.F. Wildhagen, E.W. Steyerberg, C.H. Bangma, T.H. van der Kwast, G.J. van Leenders, Cribriform growth is highly predictive for postoperative metastasis and disease-specific death in Gleason score 7 prostate cancer, Mod Pathol 28 (3) (2015) 457–464.

[6] T.A. Flood, N. Schieda, J. Sim, R.H. Breau, C. Morash, E.C. Belanger, S. J. Robertson, Evaluation of tumor morphologies and association with biochemical recurrence after radical prostatectomy in grade group 5 prostate cancer, Virchows Arch 472 (2) (2018) 205–212.

[7] N. Harding-Jackson, O.N. Kryvenko, E.E. Whittington, D.C. Eastwood, G. A. Tjionas, M. Jorda, K.A. Iczkowski, Outcome of Gleason 3 + 5 = 8 Prostate Cancer Diagnosed on Needle Biopsy: Prognostic Comparison with Gleason 4 + 4 = 8, J Urol 196 (4) (2016) 1076–1081.

[8] M.R. Downes, B. Xu, T.H. van der Kwast, Gleason grade patterns in nodal metastasis and corresponding prostatectomy specimens: impact on patient outcome, Histopathology 75 (5) (2019) 715–722.

[9] E. Hollemans, E.I. Verhoef, C.H. Bangma, J. Rietbergen, J. Helleman, M.J. Roobol, G. van Leenders, Large cribriform growth pattern identifies ISUP grade 2 prostate cancer at high risk for recurrence and metastasis, Mod Pathol 32 (1) (2019) 139–146.

[10] A.R. Rastinehad, A.A. Baccala Jr., P.H. Chung, J.M. Proano, J. Kruecker, S. Xu, J. K. Locklin, B. Turkbey, J. Shih, G. Bratslavsky, W.M. Linehan, N.D. Glossop, P. Yan, S. Kadoury, P.L. Choyke, B.J. Wood, P.A. Pinto, D'Amico risk stratification correlates with degree of suspicion of prostate cancer on multiparametric magnetic resonance imaging, J Urol 185 (3) (2011) 815–820.

[11] T. Hambrock, C. Hoeks, C. Hulsbergen-van de Kaa, T. Scheenen, J. Fütterer, S. Bouwense, I. van Oort, F. Schröder, H. Huisman, J. Barentsz, Prospective assessment of prostate cancer aggressiveness using 3-T diffusion-weighted magnetic resonance imaging-guided biopsies versus a systematic 10-core transrectal ultrasound prostate biopsy cohort, Eur Urol 61 (1) (2012) 177–184.

[12] F.H. Drost, D.F. Osses, D. Nieboer, E.W. Steyerberg, C.H. Bangma, M.J. Roobol, I. G. Schoots, Prostate MRI, with or without MRI-targeted biopsy, and systematic biopsy for detecting prostate cancer, Cochrane Database Syst Rev 4 (4) (2019) CD012663.

[13] D.J. Reesink, M.G.M. Schilham, E. van der Hoeven, I.G. Schoots, H.H.E. van Melick, R.C.N. van den Bergh, Comparison of risk-calculator and MRI and consecutive pathways as upfront stratification for prostate biopsy, World J Urol 39 (7) (2021) 2453–2461.

[14] D.F. Osses, F.H. Drost, J.F.M. Verbeek, H.B. Luiting, G. van Leenders, C.H. Bangma, G.P. Krestin, M.J. Roobol, I.G. Schoots, Prostate cancer upgrading with serial prostate magnetic resonance imaging and repeat biopsy in men on active surveillance: are confirmatory biopsies still necessary? BJU Int. 126 (1) (2020) 124–132.

[15] S. Prendeville, M. Gertner, M. Maganti, M. Pintilie, N. Perlis, A. Toi, A.J. Evans, A. Finelli, T.H. van der Kwast, S. Ghai, Role of Magnetic Resonance Imaging Targeted Biopsy in Detection of Prostate Cancer Harboring Adverse Pathological Features of Intraductal Carcinoma and Invasive Cribriform Carcinoma, J Urol 200 (1) (2018) 104–113.

[16] J. Gao, Q. Zhang, Y. Fu, W. Wang, C. Zhang, Y. Kan, H. Huang, D. Li, J. Shi, H. Guo, B. Zhang, Combined clinical characteristics and multiparametric MRI parameters for prediction of cribriform morphology in intermediate-risk prostate cancer patients, Urol Oncol 38 (4) (2020) 216–224.

[17] B. Turkbey, V.P. Shah, Y. Pang, M. Bernardo, S. Xu, J. Kruecker, J. Locklin, A. A. Baccala Jr., A.R. Rastinehad, M.J. Merino, J.H. Shih, B.J. Wood, P.A. Pinto, P. L. Choyke, Is apparent diffusion coefficient associated with clinical risk scores for prostate cancers that are visible on 3-T MR images? Radiology 258 (2) (2011) 488–495.

[18] E. Hollemans, E.I. Verhoef, C.H. Bangma, I. Schoots, J. Rietbergen, J. Helleman, M. J. Roobol, G. van Leenders, Concordance of cribriform architecture in matched prostate cancer biopsy and radical prostatectomy specimens, Histopathology 75 (3) (2019) 338–345.

[19] M. Masoomian, M.R. Downes, J. Sweet, C. Cheung, A.J. Evans, N. Fleshner, M. Maganti, T. Van der Kwast, Concordance of biopsy and prostatectomy diagnosis of intraductal and cribriform carcinoma in a prospectively collected data set, Histopathology 74 (3) (2019) 474–482.

[20] B.J. Weinreb JC, P.L. Choyke, et al., PI-RADS Prostate Imaging-Reporting and Data System, v2.1, American College of Radiology (2019).

[21] M. Truong, C. Feng, G. Hollenberg, E. Weinberg, E.M. Messing, H. Miyamoto, T. P. Frye, A Comprehensive Analysis of Cribriform Morphology on Magnetic Resonance Imaging/Ultrasound Fusion Biopsy Correlated with Radical Prostatectomy Specimens, J Urol 199 (1) (2018) 106–113.

[22] A. Arslan, D. Alis, M.B. Tuna, Y. Sağlıcan, A.R. Kural, E. Karaarslan, The visibility of prostate cancer concerning underlying histopathological variances: A single-center multiparametric magnetic resonance imaging study, Eur J Radiol 141 (2021), 109791.

[23] P.P. Tonttila, A. Ahtikoski, M. Kuisma, E. Pääkkö, P. Hirvikoski, M.H. Vaarala, Multiparametric MRI prior to radical prostatectomy identifies intraductal and cribriform growth patterns in prostate cancer, BJU Int 124 (6) (2019) 992–998.

[24] M.A. van der Slot N. Seyrek C.F. Kweldam M.A. den Bakker M.B. Busstra M. Gan S. Klaver J.B.W. Rietbergen G. van Leenders Percentage Gleason pattern 4 and PI-RADS score predict upgrading in biopsy Grade Group 2 prostate cancer patients without cribriform pattern World J Urol 40 2022 pages2723–2729.

[25] K.J. Ericson, S.S. Wu, S.D. Lundy, L.J. Thomas, E.A. Klein, J.K. McKenney, Diagnostic Accuracy of Prostate Biopsy for Detecting Cribriform Gleason Pattern 4 Carcinoma and Intraductal Carcinoma in Paired Radical Prostatectomy Specimens: Implications for Active Surveillance, J Urol 203 (2) (2020) 311–319.

[26] A. Surov, H.J. Meyer, A. Wienke, Correlations between Apparent Diffusion Coefficient and Gleason Score in Prostate Cancer: A Systematic Review, Eur Urol Oncol 3 (4) (2020) 489–497.

[27] S. Currin, T.A. Flood, S. Krishna, A. Ansari, M.D.F. McInnes, N. Schieda, Intraductal carcinoma of the prostate (IDC-P) lowers apparent diffusion coefficient (ADC) values among intermediate risk prostate cancers, J Magn Reson Imaging 50 (1) (2019) 279–287.

[28] G. van Leenders, T.H. van der Kwast, D.J. Grignon, A.J. Evans, G. Kristiansen, C.F. Kweldam, G. Litjens, J.K. McKenney, J. Melamed, N. Mottet, G.P. Paner, H. Samaratunga, I.G. Schoots, J.P. Simko, T. Tsuzuki, M. Varma, A.Y. Warren, T.M. Wheeler, S.R. Williamson, K.A. Iczkowski, The 2019 International Society of Urological Pathology (ISUP) Consensus Conference on Grading of Prostatic Carcinoma, Am J Surg Pathol 44(8) (2020) e87-e99.

[29] S. Goel, J.E. Shoag, M.D. Gross, B. Al Hussein Al Awamlh, B. Robinson, F. Khani, B. Baltich Nelson, D.J. Margolis, J.C. Hu, Concordance Between Biopsy and Radical Prostatectomy Pathology in the Era of Targeted Biopsy: A Systematic Review and Meta-analysis, Eur Urol Oncol 3 (1) (2020) 10–20.